AD-A072 634 TENNESSEE TECHNOLOGICAL UNIV COOKEVILLE DEPT OF ENGI--ETC F/G 1/3
USE OF WAGNER FUNCTIONS IN AIRFOIL DESIGN OPTIMIZATION.(U)
MAY 79 V SAHAI, C TSAO AFOSR-78-3543
UNCLASSIFIED TTU-ESM-79-2 AFOSR-TR-79-0903 NL

| OF |
AD
A072634

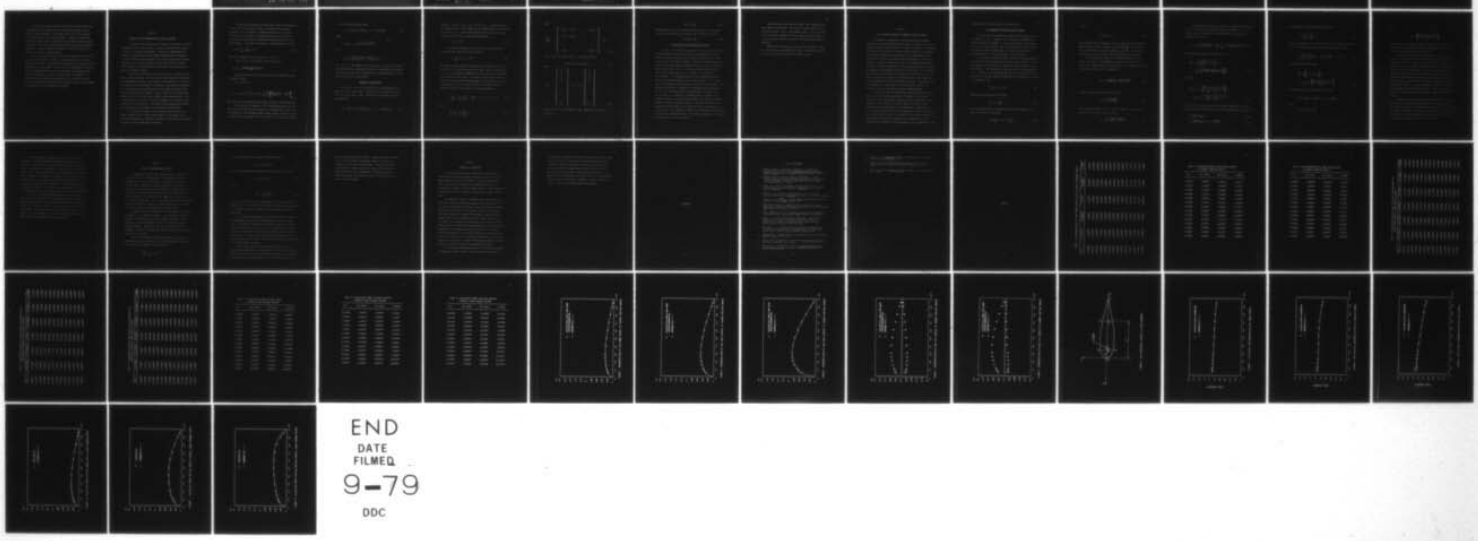

END
DATE
FILMED
9-79
DDC

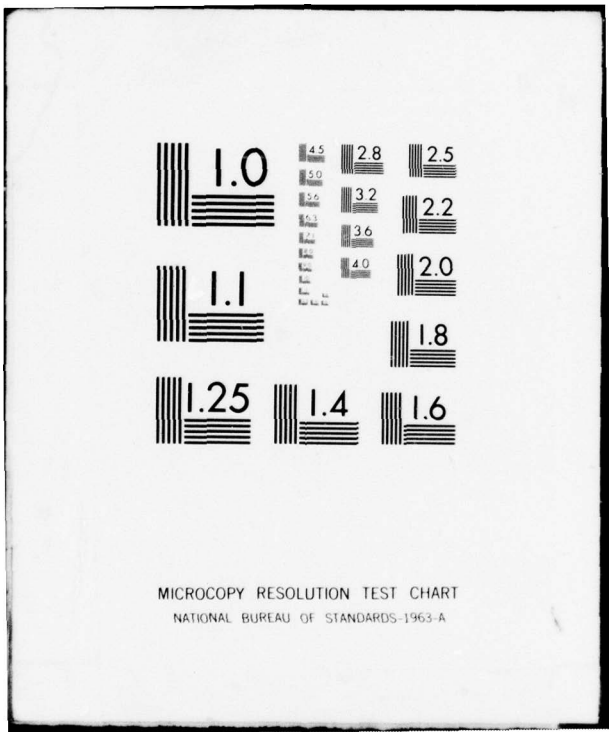
1.0
1.1
1.25
1.4
1.6
1.8
2.0
2.2
2.5
2.8
3.2
3.6
4.0
4.5
5.0
5.6
6.3
MICROCOPY RESOLUTION TEST CHART
NATIONAL BUREAU OF STANDARDS-1963-A

AFOSR-TR- 79-0903
TTU-ESM-79-2

LEVEL II

12

USE OF WAGNER FUNCTIONS IN AIRFOIL DESIGN OPTIMIZATION

VIRESHWAR SAHAI
PRINCIPAL INVESTIGATOR

AND

CHEN-PIERCE TSAO
GRADUATE ASSISTANT

Prepared For

AIR FORCE OFFICE OF SCIENTIFIC RESEARCH

BOLLING AFB
DISTRICT OF COLUMBIA
CONTRACT NUMBER AFOSR-78-3543
May 1979

TENNESSEE TECH UNIVERSITY

TENNESSEE TECHNOLOGICAL UNIVERSITY
DEPARTMENT OF ENGINEERING SCIENCE AND MECHANICS
COOKEVILLE, TENNESSEE 38501

Approved for public release; distribution unlimited

Qualified requestors may obtain additional copies from the Defense Documentation Center, all others should apply to the National Technical Information Service.

UNCLASSIFIED

SECURITY CLASSIFICATION OF THIS PAGE *(When Data Entered)*

REPORT DOCUMENTATION PAGE

READ INSTRUCTIONS BEFORE COMPLETING FORM

1. REPORT NUMBER: AFOSR-TR-79-0903	2. GOVT ACCESSION NO.
3. RECIPIENT'S CATALOG NUMBER	
4. TITLE *(and Subtitle)*: USE OF WAGNER FUNCTIONS IN AIRFOIL DESIGN OPTIMIZATION	5. TYPE OF REPORT & PERIOD COVERED: FINAL rep't. 20 Mar 78 — 19 Mar 79
	6. PERFORMING ORG. REPORT NUMBER
7. AUTHOR(s): VIRESHWAR SAHAI, CHEN-PIERCE TSAO	8. CONTRACT OR GRANT NUMBER(s): AFOSR-78-3543
9. PERFORMING ORGANIZATION NAME AND ADDRESS: TENNESSEE TECHNOLOGICAL UNIVERSITY, ENGINEERING SCIENCE & MECHANICS DEPARTMENT, COOKEVILLE, TENNESSEE 38501	10. PROGRAM ELEMENT, PROJECT, TASK AREA & WORK UNIT NUMBERS: 2307D9, 61102F
11. CONTROLLING OFFICE NAME AND ADDRESS: AIR FORCE OFFICE OF SCIENTIFIC RESEARCH/NA, BLDG 410, BOLLING AIR FORCE BASE, D C 20332	12. REPORT DATE: May 1979 13. NUMBER OF PAGES: 52
14. MONITORING AGENCY NAME & ADDRESS *(if different from Controlling Office)*: TTU-ESM-79-2	15. SECURITY CLASS. *(of this report)*: UNCLASSIFIED 15a. DECLASSIFICATION/DOWNGRADING SCHEDULE

16. DISTRIBUTION STATEMENT *(of this Report)*

Approved for public release; distribution unlimited.

17. DISTRIBUTION STATEMENT *(of the abstract entered in Block 20, If different from Report)*

18. SUPPLEMENTARY NOTES

19. KEY WORDS *(Continue on reverse side if necessary and identify by block number)*

Airfoil profiles, Wagner functions, subsonic airfoil design

20. ABSTRACT *(Continue on reverse side if necessary and identify by block number)*

The feasibility of using a series of Wagner functions to represent airfoil contours in design procedures has been investigated. It was demonstrated that a large class of airfoils can be adequately described by a relatively small number of terms. A least squares type of procedure was used to determine the unknown coefficients in the series representation. The use of Wagner function representation in thin symmetrical airfoil design was investigated. Both the direct method of analysis in which the velocity distribution is calculated for a known shape and the inverse method of design in which the airfoil shape corresponding

DD FORM 1 JAN 73 1473

UNCLASSIFIED

407 776

to a specified velocity distribution is determined were considered. Standard airfoil data was used to test the suitability of the Wagner function representation, and the results were found to be satisfactory. Rapid calculations were possible even in the inverse mode since the use of Wagner functions allowed the determination of all the improper integrals that appear in thin airfoil theory in closed form.

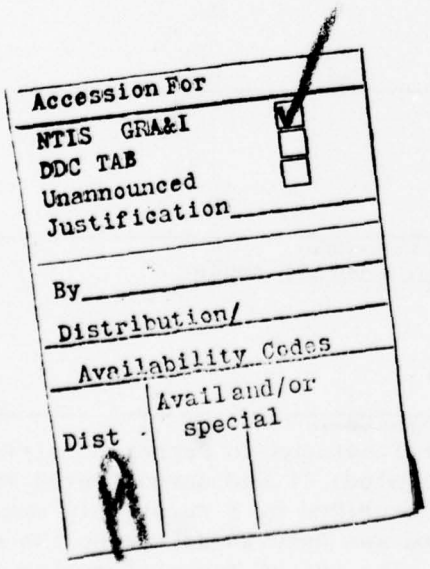

Conditions of Reproduction

Reproduction, translation, publication, use and disposal in whole or in part by or for the United States Government is permitted.

AIR FORCE OFFICE OF SCIENTIFIC RESEARCH (AFSC)
NOTICE OF TRANSMITTAL TO DDC
This technical report has been reviewed and is approved for public release IAW AFR 190-12 (7b).
Distribution is unlimited.
A. D. BLOSE
Technical Information Officer

USE OF WAGNER FUNCTIONS
IN AIRFOIL DESIGN OPTIMIZATION

VIRESHWAR SAHAI

PRINCIPAL INVESTIGATOR

and

CHEN-PIERCE TSAO

GRADUATE ASSISTANT

Prepared For

AIR FORCE OFFICE OF SCIENTIFIC RESEARCH

BOLLING AFB

DISTRICT OF COLUMBIA

CONTRACT NUMBER AFOSR-78-3543

MAY 1979

TENNESSEE TECHNOLOGICAL UNIVERSITY

DEPARTMENT OF ENGINEERING SCIENCE AND MECHANICS

COOKEVILLE, TENNESSEE 38501

ABSTRACT

The feasibility of using a series of Wagner functions to represent airfoil contours in design procedures has been investigated. It was demonstrated that a large class of airfoils can be adequately described by a relatively small number of terms. A least squares type of procedure was used to determine the unknown coefficients in the series representation. The use of Wagner function representation in thin symmetrical airfoil design was investigated. Both the direct method of analysis in which the velocity distribution is calculated for a known shape and the inverse method of design in which the airfoil shape corresponding to a specified velocity distribution is determined were considered. Standard airfoil data was used to test the suitability of the Wagner function representation, and the results were found to be satisfactory. Rapid calculations were possible even in the inverse mode since the use of Wagner functions allowed the determination of all the improper integrals that appear in thin airfoil theory in closed form.

TABLE OF CONTENTS

LIST OF TABLES

LIST OF FIGURES

Section I

INTRODUCTION

There are two types of numerical procedures available for the design of airfoils. In one technique, called the direct method, the flow about a prescribed airfoil is analyzed; and then, based upon this result, the airfoil shape is modified in an attempt to satisfy the design conditions. The other design formulation is the inverse method in which the airfoil surface pressures or velocities are specified, and the airfoil shape is subsequently determined. The design is usually optimized subject to specified aerodynamic and structural constraints.

There have been many recent attempts to computerize airfoil design procedure. Barger and Brooks [1] used a streamline curvature method to design airfoils. This method is based on the Theodoreson Transformation, which requires complicated conformal mappings for the representation of the airfoil geometry. After the airfoil is tailored to obtain the desired pressure distribution, the contour has to be adjusted to satisfy the proper trailing edge conditions. TSFOIL code [2] has recently been developed for the analysis and design of two-dimensional transonic airfoils. It is capable of computing both free-air flows and flows under various wind-tunnel wall conditions. The implementation of TSFOIL requires the specification of the airfoil geometry, preferably in a suitable functional form. Other design methods of note are the inverse methods of Beatty and Narromore [3] and Carlson [4]. Most of these codes are based on the inviscid theory. The usual approach for taking viscous effects into account

is to treat the airfoil determined by the inviscid design method as the displacement surface and to subtract from it the displacement thickness determined by a boundary layer computation. The latest version of the Carlson's code [5], for example, accounts for the viscous effects in this manner.

An important advantage to the computational method is that it allows the use of numerical optimization techniques for automated airfoil design. Vanderplaats, Hicks and Murman [6] have investigated one such method which uses direct optimization for two dimensional flow. They have developed a numerical optimization design code by linking an optimization program based on the method of feasible directions with an aerodynamic analysis program that uses a relaxation method to solve the partial differential equations governing inviscid, small disturbance flow. Hicks and Szelazek [7] have recently developed a similar technique for design of subsonic airfoils using a minicomputer. The numerical optimization technique involves the minimization of some specified parameter, such as the lift coefficient, for a set of design parameters describing the airfoil geometry and satisfying a number of specified constraints. A weak point of this analysis is probably the use of a simple polynomial contour representation, since it somewhat limits the class of obtainable solutions.

A second procedure being developed at the National Aerospace Laboratory in the Netherlands and described briefly by Sloof [8] is the so-called constrained inverse method. In this procedure, a least squares technique is used for the design problem in such a manner that an a priori specified balance is obtained between the prescribed pressure distribution and the geometric requirements. Labrujere [9] has applied this technique to the two-dimensional incompressible flow problem.

The design procedures mentioned above are only a small sample of a large number of such methods which have already been developed or are currently under development. An important first step in these methods is the specification of the airfoil geometry. Ideally, the functional relationship chosen should be numerically well conditioned and be capable of modeling a wide range of airfoil shapes while maintaining computational efficiency. It seems worthwhile, therefore, to search for and test new functions to represent airfoil geometry.

The functional relationship proposed here requires the expression of the slope of the airfoils in terms of a Fourier series of the so-called Wagner functions [10]. This proposed representation of the airfoil contour, described in the next chapter, seems to meet the requirements stated above. It will be demonstrated that it has the capability of generating a wide class of airfoil shapes in terms of a small number of parameters. In addition, the Wagner function representation will be used in an inverse type of procedure using thin airfoil theory and the results will be compared with available data for standard airfoil shapes.

Section 2

WAGNER FUNCTION REPRESENTATION OF AIRFOIL CONTOURS

In an airfoil design procedure, the contour of the airfoil is usually represented in one of the two ways. One way is to represent the contour by means of a polygonal-shaped figure. This type of representation is suitable for computations by direct method using both finite difference and finite element procedures because of the ease in applying the boundary conditions. In an inverse procedure, however, this may lead to shapes that correspond to the given pressure distributions but are unacceptable from the structural viewpoint.

Another way of representing the airfoil contour is to express it in terms of simple functions. The functions used most commonly are polynomial and trigonometric functions. The polynomial representation is, by far, the most popular but has the drawback of requiring a large number of parameters. It is unsuitable for the representation of some shapes and requires geometrical constraints (for example, to obtain closure at the trailing edge). Fourier Sine series are also used in airfoil contour representation. Such a representation allows the use of Glauert integrals in the classical thin airfoil theory (see Section 3). The Fourier series representation suffers from somewhat the same drawbacks as the polynomial representation.

It is obvious, therefore, that the computational efficiency of a design procedure will be enhanced significantly, if the airfoil can be represented adequately by a function in terms of a small number of parameters and without requiring additional constraints.

The functional relationship proposed here requires the expression of the slope of the airfoil in terms of a Fourier series of Wagner functions. Let the contour of a symmetrical airfoil be the equation $y = f(x)$ $(o \leq x \leq 1)$ where x is measured along the chord of the airfoil and both coordinates are non-dimensionalized with respect to the chord length c. The slope of the airfoil is then expressed as follows:

$$f'(x) = \sum_{n=1}^{\infty} A_n W_n(\theta) - A_0 \tag{2.1}$$

where θ is related to x by the equation $x = \sin^2 \theta/2$.

$W_n(\theta)$ are the so-called Wagner functions given by

$$W_n(\theta) = \frac{2}{\pi} \frac{\cos[(n + 1)\theta] + \cos n\theta}{\sin\theta} \tag{2.2}$$

The above equation for the slope can be easily integrated to give the airfoil contour.

It is given by

$$y = - A_o \sin^2 \frac{\theta}{2} + \frac{A_0}{\pi} (\theta + \sin\theta) + \sum_{n=1}^{\infty} \frac{A_n}{\pi} \left[\frac{\sin(n + 1)\theta}{n + 1} + \frac{\sin n\theta}{n} \right] \tag{2.3}$$

Note that the above expansion itself ensures closure at the trailing edge.

The suitability of equation (2.3) in representing airfoil contours will be tested by fitting this expression to standard airfoil shapes. For this purpose, the data for NACA 4-digit airfoil profiles [11] will be used. In order to fit the equation (2.3) to this data, it is convenient to write

it in the following discrete form:

$$Y_i = F_0(\theta_i)A_0 + F_1(\theta_i)A_1 + \text{-----} + F_n(\theta_i)A_n \qquad (2.4)$$

where

$$F_0(\theta_i) = -\sin^2\frac{\theta_i}{2} + \frac{\theta_i + \sin\theta_i}{\pi},$$

and

$$F_n(\theta_i) = \left[\frac{\sin(n+1)\theta_i}{n+1} + \frac{\sin n\theta_i}{n}\right] /\pi,$$

(n = 1, 2, --). The problem is to find A_0, A_1------, A_n so that equation (2.3) will best fit a given airfoil profile. The method of least squares [12] will be used here for this purpose and a brief introduction to this method is given in the next section.

Method of Least Squares

Let there be a set of n data points (X_i, Y_i) through which it is desired to pass a certain curve. This curve is to represent the "best fit" in the least squares sense. Equation (2.4) is rewritten in the following form:

$$\overline{Y}_i = A_1^* F_1^*(\theta_i) + A_2^* F_2^*(\theta_i) + \text{--------} + A_j^* F_j^*(\theta_i) \qquad (2.5)$$

where $A_1^* = A_0$, $A_j^* = A_{j+1}$, $F_1^* = F_0$, $F_j^* = F_{j+1}$, and $\bar{Y}_i$ represents the calculated value of the ordinate by the Wagner function representation for the ith point. If the actual ordinate of this point is Y_i, then the error of fit at the ith point can be defined as

$$E_i = Y_i - \bar{Y}_i \tag{2.6}$$

The sum of the squares of errors at all of the data points is called the total error of fit and is given by

$$S = \sum_{i=1}^{n} E_i^2 = (Y_i - \bar{Y}_i)^2 \tag{2.7}$$

The errors have been squared to eliminate possible cancellation. The total error is a function of how well the curve "fits" the data points; i. e., it is a function of parameters A_n^* which control the positioning of the curve in the X-Y plane. It should be fairly evident that the "best" fit is that position which minimizes the total error. To find this position, let S be a function of A_n^*'s and require that its derivatives vanish. This leads to the following equations

$$\frac{\partial S}{\partial A_j^*} = \frac{\partial}{\partial A_j^*} \sum_{i=1}^{n} (Y_i - \bar{Y}_i)^2 = 0, \quad j = 1, 2 \text{ -------- } n \tag{2.8}$$

or,

$$\sum_{i=1}^{n} (Y_i - \bar{Y}_i) \frac{\partial \bar{Y}_i}{\partial A_j^*} = 0 \tag{2.9}$$

where

$$\frac{\partial \bar{Y}_i}{\partial A_j^*} = \begin{bmatrix} F_1(\theta_1) & F_2(\theta_1) & \cdots & F_n(\theta_1) \\ F_1(\theta_2) & F_2(\theta_2) & & \\ \vdots & & & \\ F_1(\theta_m) & \cdots & & F_n(\theta_m) \end{bmatrix} = [F] \qquad (2.10)$$

Equation (2.9) can then be written in the matrix form as

$$[F]^t [Y] - [F]^t [F] [A] = 0 \qquad (2.11)$$

where

$$[A] = \begin{bmatrix} A_1^* \\ A_2^* \\ A_3^* \\ \vdots \\ A_n^* \end{bmatrix} \quad \text{and} \quad [Y] = \begin{bmatrix} Y_1 \\ Y_2 \\ Y_3 \\ \vdots \\ Y_m \end{bmatrix} \qquad (2.12)$$

Letting $[F]^t [F] = [C]$ and $[F]^t [Y] = [B]$. Equation (2.11) can then be written as

$$[B] = [C]\,[A] \tag{2.13}$$

Multiplying both sides of the above equation, by $[C]^{-1}$, the described coefficient matrix [A] for the best fit can be obtained as follows:

$$[C]^{-1}[B] = [A] \tag{2.14}$$

Representation of Standard Airfoil Shapes

The use of the method of least squares will now be illustrated by fitting the Wagner function representation to the NACA 0006 airfoil. Table 1 gives the actual value of the ordinates (taken from Ref. [11]) of this airfoil for various chordwise locations. Truncated form of the Wagner function representation (equation (2.4)) was used in fitting the airfoil contour data. For n = 2, the least squares method gives the values of the coefficients as $A_0 = 0.071049$, $A_1 = 0.011098$, and $A_2 = 0.0051307$. The calculated values for each chordwise position as well as the percentage errors are also given in Table 1. It is noted that at the leading and trailing edges the errors are fairly large. Considerable improvement is obtained by considering a four-term expansion (n = 3). The calculated values of the coefficients in the case are: $A_0 = 0.10148$, $A_1 = 0.019233$, $A_2 = 0.0044033$ and $A_3 = 0.008108$. The percentage errors in representing the contour of the airfoil at various chordwise locations are shown in Table 1. This time the error at the leading and trailing edges is less than 1.5%, and is considereably less at other places. This accuracy is deemed to be sufficient for representing the shape of the NACA 0006 airfoil. The graphical comparison of calculated and actual shapes is shown in Figure 1.

Computations were also made for several other standard airfoil shapes (NACA 0010 and 0018). The results for these computations are presented in Tables 2 and 3 and Figures 2 and 3. It is clear from these results that a variety of airfoil shapes can be represented by a series of Wagner function in terms of a relatively small number of parameters.

Wagner function series may also be used to represent the upper and lower surface of an unsymmetrical airfoil. The results for NACA 2412 and 4412 airfoils are presented in Figure 4 and 5.

Section 3

USE OF WAGNER FUNCTIONS IN SYMMETRICAL AIRFOIL DESIGN

The problem of calculating the flow field and the aerodynamic properties of any given arbitrary airfoil with no restrictions as to its thickness, camber or angle of attack is complex in practice. The available methods are not convenient for either a rapid estimation of the velocity or pressure distribution over the airfoil or for designing an airfoil profile that will have a prescribed surface distribution of velocity or pressure. In order to demonstrate the use of the Wagner function representation, it will be advantageous to have an approach that will in some way simplify the mathematical conditions of the problem. Such an alternative approach is provided by the classical thin airfoil theory. In this theory, the airfoil is assumed to be sufficiently thin and elongated so that the assumption of small perturbation can be made. Even though such an assumption is not valid near the leading edge of an airfoil, the solution of the resulting simple problem is remarkably useful.

The details of the thin airfoil theory may be found in Reference [13]. Both the governing equations and the boundary conditions are linearized in this theory, thus allowing the use of superposition. The problem of a thin airfoil at a non-zero angle of attack can then be represented as the superposition of the problem for a symmetrical airfoil at zero incidence and that for a cambered airfoil with zero thickness at a non-zero angle of attack. The solution of these two problems may be accomplished by the method of superposition of singularities. The application of the Wagner function representation to the symmetrical airfoil

design using thin airfoil theory is discussed below.

Thin Symmetrical Airfoil at Zero Incidence

The flow past a thin symmetrical airfoil at zero angle of attack (see Figure 6) can be simulated by a continuous distribution of sources and sinks, of strength $\sigma = \sigma(x)$ per unit length located along the chord line of the airfoil. Here x is the distance along the chord line measured from the leading edge. An element of length δx has associated with it a source of strength $\sigma \cdot \delta x$ on the x-axis.

In the context of the thin airfoil theory, the flow perturbations are assumed to be small compared with the free stream velocity V. Also, the thickness of the airfoil is considered to be small compared to the chord length c. The flux across a line such as PQ is then approximately $V \cdot 2y$. However, all the fluid generated by the sources between O and N must cross the line PQ, because the part POQ of the boundary of the airfoil is a streamline. Thus

$$\int_0^x \sigma(x) \cdot dx = 2Vy \tag{3.1}$$

Differentiating with respect to x yields

$$\sigma(x) = 2V \cdot \frac{dy}{dx} \tag{3.2}$$

Thus the required source of distribution is simply determined by the shape of the airfoil. Note that

$$\int_0^c 2V \frac{dy}{dx} dx = 2V \cdot [y]_{x=0}^{x=c} = 0 \tag{3.3}$$

so that

$$\int_0^c \sigma(X)\, dx = 0 \tag{3.4}$$

which confirms that the algebraic sum of the source and sink strengths within the body is zero. Further, at places where $\frac{dy}{dx} > o$, i.e., at the front of the airfoil, the source strength is positive. At the rear of the airfoil, on the other hand, there are negative sources (sinks).

In this first order theory, the velocity perturbation at the point P' in Figure 6 is approximately the same as the point N' on the x-axis, and is denoted by u_p' in the x-direction. The component at P' due to the source $\sigma(x)\, dx$ at N is then given by

$$du_p' = \frac{\sigma\,(x)\, dx}{2\pi\,(x - x')} = \frac{2V\, f'\,(x)\, dx}{2\pi\,(x - x')} \tag{3.5}$$

The total perturbation velocity at P' is then

$$u_p' = \frac{V}{\pi} \int_0^c \frac{f'(x)\, dx}{(x - x')} \tag{3.6}$$

It is convenient to let $x = \frac{1}{2}\, c\, (1 - \cos\theta)$. Then $dx = \frac{1}{2}\, c \sin\theta\ d\theta$, and $(x - x') = \frac{1}{2}c\, (\cos\theta - \cos\theta)$, so that

$$u_p' = \frac{V}{\pi} \int_0^{\pi} \frac{f'\,(\theta) \cdot \sin\theta\, d\theta}{(\cos\theta\ - \cos\,\theta')} \tag{3.7}$$

The perturbation velocity u_p' can thus be calculated from equation (3.7) if the slope of the airfoil is known as a function of θ. If the airfoil contour is described by the Wagner function representation [equation (2.3)], then

$$f'(\theta) = A_0 \left[\frac{2(1 + \cos\theta)}{\sin\theta} - 1 \right] + \frac{2}{\pi} \sum_{n=1}^{\infty} An \frac{\cos[(n + 1)\theta] + \cos\theta}{\sin\theta} \tag{3.8}$$

The perturbation velocity is then given by

$$\frac{u_p'}{V} = \frac{1}{\pi} \int_0^{\pi} \left\{ A_0 \left[\frac{2(1 + \cos\theta)}{\pi} \right] - \sin\theta + \frac{2}{\pi} \sum_{n=1}^{\infty} A_n \left[\frac{\cos[(n + 1)\theta] + \cos n\theta}{\cos\theta - \cos\theta'} \right] \right\} d\theta \tag{3.9}$$

for which

$$\frac{u_p'}{V} = A_0 \cdot \frac{1}{\pi} \int_0^{\pi} \left[\frac{2(1 + \cos\theta)/\pi - \sin\theta}{\cos\theta - \cos\theta'} \right] d\theta + \sum_{n=1}^{\infty} A_n \frac{2}{\pi} \int_0^{\pi} \frac{\cos[(n + 1)\theta] + \cos n\theta}{\cos\theta - \cos\theta'} d\theta \tag{3.10}$$

Except for the second term, all of the integrals appearing on the right hand side can be determined by means of the following Glauert integrals [13]

$$\int_0^{\pi} \frac{d\theta}{\cos\theta - \cos\theta'} = 0 \tag{3.11a}$$

$$\int_0^{\pi} \frac{\cos n\theta}{\cos\theta - \cos\theta'} d\theta = \pi \cdot \frac{\sin n\theta'}{\sin\theta} \tag{3.11b}$$

The integral in the second term can be written as

$$\int_0^{\pi} \frac{\sin\theta - \sin\theta'}{\cos\theta - \cos\theta'} \, d\theta \tag{3.12}$$

Since the contribution due to the $\sin\theta'$ term is zero because of equation (3.11a), the integral (3.12) can easily be evaluated as follows:

$$\int_0^{\pi} \frac{\sin\theta - \sin\theta'}{\cos\theta - \cos\theta'} \, d\theta = -\int_0^{\pi} \cot\left(\frac{\theta+\theta'}{2}\right) d\theta = 2 \ln \tan \frac{\theta'}{2} \tag{3.13}$$

The equation (3.10) then becomes

$$\frac{u_p'}{V} = A_0\left[\frac{2}{\pi} + \frac{2}{\pi} \ln \tan \frac{\theta}{2}\right] + \sum_{n=1}^{\infty} A_n \frac{2}{\pi} \left[\frac{\sin (n+1)\theta' + \sin n\theta'}{\sin\theta'}\right] \tag{3.14}$$

The above equation can be rewritten in the form

$$\frac{u_p'}{V} = A_0 F_0'(\theta') + A_1 F_1'(\theta') + \text{----} + A_n F_n'(\theta') \tag{3.15}$$

where

$$F_0' = \frac{2}{\pi} + \frac{2}{\pi} \ln \tan \frac{\theta'}{2}$$

and

$$F_n' = \frac{2}{\pi}\left[\frac{\sin (n+1)\theta' + \sin n\theta'}{\sin \theta'}\right]$$

If the values of the Wagner coefficients (A's) are known for a given airfoil, then the perturbation velocity corresponding to a given θ' can be determined easily from equation (3.15).

For NACA 0006 airfoil, the coefficients A's were calculated in Chapter 2 by using the known contour of the airfoil. The perturbation velocities can then be evaluated at various chordwise locations by using equation (3.15). The reference data [11] as well as the calculated values are given in Table 4 and Figure 7. The error in total velocity and pressure is of the order of one percent for this 6% thick airfoil. Similar calculations were also made for NACA 0010-64 and 0018 airfoils and the results are given in Table 5 (Figure 8) and Table 6 (Figure 9), respectively. There is a considerable amount of error at the leading and trailing edges for the NACA 0018 airfoil. This is to be expected since thin airfoil theory is being used for a moderately thick (18%) airfoil.

Equation (3.15) can also be used in an inverse type of procedure which is more useful from a design standpoint. The airfoil designer often wants to determine the contour that will produce a desired velocity or pressure distribution. He may want a particular type of distribution, for instance, so that the airfoil will have favorable boundary layer characteristics (delayed separation, low drag, etc.).

The coefficients A_n in equation (3.15) are the same as those appearing in the Wagner function representation of the airfoil profile as given by equation (2.3). Once these coefficients are determined, the shape of the airfoil that corresponds to a given velocity distribution becomes known. Comparing equation (3.15) with equation (2.6), which was used to determine the coefficients in Wagner series representation of an airfoil by the least squares method, one may observe that the two equations are essentially of the same form. The least squares method, as described in Chapter 2, can also be used to determine the coefficients A_n in equation (3.15) that correspond to a specified velocity distribution.

The inverse procedure described above was tested by using the known velocity distributions for standard airfoil shapes to determine the corresponding contours. The results for NACA 0006, 0010-64 and 0010-66 airfoils are presented in Tables 7, 8 and 9 (Figures 10, 11, and 12), respectively. The calculations were performed for the case n = 3. The errors at the trailing edge can be improved somewhat by using a larger number of terms in the Wagner series representation.

Section 4

DESIGN OF NONSYMMETRICAL AIRFOILS

A symmetrical airfoil at zero angle of attack is incapable of producing any lift or pitching moment. As indicated in Chapter 3, a cambered airfoil can be represented as a mean camber line of zero thickness with a symmetrical thickness distribution superimposed on it. Within the context of the thin airfoil theory, the induced velocity at any point of the cambered airfoil may be found by superimposing the induced velocity at the point due to the camber line and that due to the thickness distribution. Just as the summetrical airfoil was analyzed using a distribution of sources, the induced velocity due to a camber line may be calculated by replacing it by a vortex system.

A camber line can be represented by the same shape as that shown in Figure 6 for a symmetrical airfoil. It is unsuitable, however, to represent the camber line by a series of Wagner functions. It was found that such a representation requires the evaluation of highly singular integrals. Camber lines are best represented by means of piecewise polynomials. Standard NACA camber line shapes, for example, are built in this manner.

Allen [14] showed that the load distribution and the slope of the camber line can be represented in terms of conjugate Fourier series. If the slope of the camber line is represented as

$$\frac{dy_c}{dx} = \sum_{n=1}^{\infty} b_n \cos n\theta \qquad (4.1)$$

the lift coefficient at zero angle of attack is given by

$$C_{L,0} = \pi (2B_0 + B_1) \tag{4.2}$$

and the pitching-moment coefficient about the quarter-chord point is

$$C_m = \frac{\pi}{4} (B_2 - B_1) \tag{4.3}$$

where

$$B_0 = -\frac{1}{\pi} \int_0^{\pi} \frac{dy_c}{dx} \, d\theta \tag{4.4}$$

and B_1 and B_2 are the first two coefficients in the Fourier series of Equation (4.1). Von Mises [15] has suggested a simple way of calculating the coefficients B_n when the camber line is represented in terms of polynomials.

It is apparent from Equations (4.1) and (4.2) that the lift and pitching-moment coefficients are controlled by B_1 and B_2. A camber line could therefore be designed by specifying B_1 and B_2 in accordance with the desired values of $C_{L,0}$ and C_m. For a camber line so obtained, a family of airfoils can be generated by specifying various thickness distributions. As shown earlier, the velocity and pressure due to this added symmetrical profile can be calculated expeditiously by representing it in terms of Wagner functions.

The design procedure described above seems to be especially suitable for implementation on a minicomputer. The method is, of course, limited by the assumptions of the thin airfoil theory. These assumptions are violated over the entire airfoil if it is sufficiently thick and

near the leading edge for any airfoil. Nevertheless, this procedure can be used to determine a preliminary design to be refined, if necessary, by more sophisticated methods. These methods consume a large amount of computer time in the inverse mode and require a large computer for their implementation. Considerable amount of savings in computer time should be possible if the initial input is close to the final design.

Section 5

SUMMARY AND CONCLUSIONS

The purpose of the present research was to investigate the feasibility of representing airfoil contours in terms of a series of Wagner functions in airfoil procedures. It has been demonstrated that a large class of airfoils can be adequately described by a relatively small number of terms of Wagner series. A least squares type of procedure was used to determine the unknown coefficients of these terms.

For symmetrical airfoils, the Wagner series representation was found to be especially useful when using the thin airfoil theory. It is possible to determine the principal value of the improper integrals that appear in this theory in closed form. Thus the long computer time usually required to evaluate such integrals numerically can be avoided. Both the direct method of analysis in which the velocity distribution is calculated for a known shape and the inverse method of design in which the airfoil shape corresponding to a specified velocity distribution is determined are presented in Section 3. The Wagner function representation of the airfoil allows fast calculations even in the inverse mode since it is possible to evaluate all the improper integrals in closed form. A method of designing nonsymmetrical airfoils based on thin airfoil theory has been suggested in Section 4.

It is concluded that Wagner functions are suitable for representing symmetrical airfoil contours. They are not suited, however, for

representation of camber lines since, at least in thin airfoil theory, their use leads to the necessity of evaluating singular integrals. In principle, Wagner functions can be used to represent the upper and lower surfaces of nonsymmetrical airfoils, but their use in methods involving thick airfoil theory needs investigation. The Wagner function representation also seems suitable for design methods having a boundary layer analysis capability. Finally, their use in transonic airfoil design methods merits investigation.

REFERENCES

LIST OF REFERENCES

1. Barger, Raymond L. and Cuyler W. Brooks, Jr., "Computerized Procedures for Airfoil Design," Aerodynamic Analysis Requiring Advanced Computers, Part II, NASA, sp-347, March 1975, pp. 703-712.

2. Murman, Earell M., Frank R. Bailey, and Margaret L. Johnson, "TSFOIL-A Computer Code for Two-dimensional Transonic Calculations, Including Wind-Tunnel Effects and Wave-Drag Evaluation," NASA, sp-347, March 1975, pp. 769-788.

3. Beatty, T. D. and J. C. Narramore, "Inverse Method for the Design of Multielement High-Lift Systems," J. Aircraft, vol. 13, No. 6, 1976, pp. 393-398.

4. Carlson, L. A., "Transonic Airfoil Analysis and Design Using Carlesian Coordinates," J. Aircraft, vol. 13, no. 5, 1976, pp. 349-356.

5. Carlson, L. A., "TRANDES: A Fortran Program for Transonic Airfoil Analysis or Design," NASA, CR-2821, 1977.

6. Vanderplaats, Garret N., Raymond N. Hicks, and Earll M. Murman, "Application of Numerical Optimization Techniques to Airfoil Design," NASA, sp-347, March 1975, pp. 749-768.

7. Hicks, Raymond M. and C. A. Szelazek, "Airfoil Design by Numerical Optimization Using a Minicomputer," NASA, TM-78502. December 1978.

8. Sloof, J. M., "Wind Tunnel Tests and Aerodynamic Computations: Thoughts on Their Use in Aerodynamic Design," presented at the AGARD Meeting on Numerical Methods and Wind Tunnel Testing, Rhode-St-Genese, Belgium, June 23-24, 1976.

9. Labrujere, T. E., "Airfoil Design by the Method of Singularities Via Parametric Optimization of a Geometrically Constrained Least Squares Object Function," NLR, TR-76139U, November, 1976.

10. Ramamoorthy, P., "Wagner Functions," National Aeronautical Laboratory, Bangalore, NAL, TN 16, 1969.

11. Abbott, Ira H. and Albert E. Von Doenhoff, Theory of Wing Sections. New York: McGraw-Hill, Inc., 1970.

12. Pipes, Louis A. and Lawrence R. Harvill, Applied Mathematics for Engineers and Physicists. New York: McGraw-Hill, Inc., 1970.

13. Clancy, L. J., Aerodynamics. New York: Halsted Press, a division of John Wiley & Sons, Inc., 1975.

14. Allen, H. Julian, "General Theory of Airfoil Sections Having Arbitrary Shape or Pressure Distribution," NASA, Rep. No. 833, 1945.

15. Mises, Richard Von, Theory of Flight. New York: Dover Publications, Inc., 1959.

APPENDIX

TABLE 1. REPRESENTATION OF NACA 0006 AIRFOIL USING WAGNER FUNCTION SERIES

X/C	Y/C (REF)	Y/C (CAL) (N=2)	% ERROR	Y/C (CAL) (N=3)	% ERROR
0.05000	0.01777	0.01826	2.75183	0.01803	1.45751
0.07500	0.02100	0.02130	1.43810	0.02107	0.33333
0.10000	0.02341	0.02354	0.55105	0.02336	0.23494
0.15000	0.02673	0.02658	0.55743	0.02656	0.63973
0.20000	0.02869	0.02840	1.01081	0.02855	0.50192
0.25000	0.02971	0.02939	1.08381	0.02965	0.20195
0.30000	0.03001	0.02974	0.88637	0.03005	0.13329
0.40000	0.02902	0.02899	0.09993	0.02917	0.52033
0.50000	0.02647	0.02669	0.84246	0.02658	0.42312
0.60000	0.02282	0.02315	1.42419	0.02279	0.11394
0.70000	0.01832	0.01854	1.22817	0.01821	0.62773
0.80000	0.01312	0.01305	0.50305	0.01306	0.44970
0.90000	0.00724	0.00682	5.81215	0.00731	0.96409
0.95000	0.00403	0.00347	13.81886	0.00401	0.49380

TABLE 2. REPRESENTATION OF NACA 0010 AIRFOIL BY WAGNER FUNCTION SERIES

X/C	Y/C (REF)	Y/C (CAL)	% ERROR
0.05000	0.02962	0.03005	1.45172
0.07500	0.03500	0.03512	0.33429
0.10000	0.03902	0.03893	0.23834
0.15000	0.04455	0.04427	0.63300
0.20000	0.04782	0.04758	0.50397
0.25000	0.04952	0.04942	0.19992
0.30000	0.05002	0.05009	0.13395
0.40000	0.04837	0.04862	0.51892
0.50000	0.04412	0.04430	0.41704
0.60000	0.03803	0.03799	0.11044
0.70000	0.03053	0.03034	0.62234
0.80000	0.02187	0.02177	0.46182
0.90000	0.01207	0.01219	0.96935
0.95000	0.00672	0.00669	0.48661

TABLE 3. REPRESENTATION OF NACA 0018 AIRFOIL BY WAGNER FUNCTION SERIES

X/C	Y/C (REF)	Y/C (CAL)	% ERROR
0.05000	0.05332	0.05409	1.44599
0.07500	0.06300	0.06321	0.33492
0.10000	0.07024	0.07007	0.24630
0.15000	0.08018	0.07968	0.62859
0.20000	0.08606	0.08563	0.49617
0.25000	0.08912	0.08895	0.19524
0.30000	0.09003	0.09014	0.12551
0.40000	0.08705	0.08750	0.52154
0.50000	0.07941	0.07974	0.41431
0.60000	0.06845	0.06837	0.11103
0.70000	0.05496	0.05461	0.63501
0.80000	0.03935	0.03918	0.42694
0.90000	0.02172	0.02193	0.97145
0.95000	0.01210	0.01203	0.56198

TABLE 4. CALCULATED VELOCITY AND PRESSURE DISTRIBUTION FOR NACA 0006 AIRFOIL USING DIRECT METHOD

X/C	VEL (REF)	VEL (CAL)	% ERROR	PR (REF)	PR (CAL)	% ERROR
0.05000	1.10300	1.11350	0.95195	1.21700	1.23980	1.87346
0.07500	1.10700	1.10500	0.18067	1.22500	1.22110	0.31837
0.10000	1.10100	1.09980	0.10899	1.21200	1.20960	0.19802
0.15000	1.09800	1.09320	0.43716	1.20600	1.19500	0.91211
0.20000	1.09100	1.08830	0.24748	1.19000	1.18430	0.47899
0.25000	1.08600	1.08360	0.22099	1.17900	1.17420	0.40712
0.30000	1.07800	1.07870	0.06494	1.16200	1.16360	0.13769
0.40000	1.06600	1.06750	0.14071	1.13600	1.13960	0.31690
0.50000	1.05300	1.05480	0.17094	1.10900	1.11250	0.31560
0.60000	1.04200	1.04120	0.07678	1.08600	1.08420	0.16575
0.70000	1.02800	1.02770	0.02918	1.05700	1.05620	0.07569
0.80000	1.01300	1.01430	0.12833	1.02600	1.02890	0.28265
0.90000	0.99000	0.99740	0.74747	0.98000	0.99481	1.51122
0.95000	0.97400	0.98048	0.66530	0.94900	0.96134	1.30032

TABLE 5. CALCULATED VELOCITY AND PRESSURE DISTRIBUTION FOR NACA 0010-64 AIRFOIL USING DIRECT METHOD

X/C	VEL (REF)	VEL (CAL)	% ERROR	PR (REF)	PR (CAL)	% ERROR
0.05000	1.13400	1.16040	2.32804	1.28600	1.34640	4.69673
0.07500	1.13000	1.14440	1.27434	1.27700	1.30960	2.55286
0.10000	1.12700	1.13500	0.70985	1.26900	1.28830	1.52088
0.15000	1.12300	1.12520	0.19590	1.26100	1.26620	0.41237
0.20000	1.11700	1.12080	0.34020	1.24800	1.25610	0.64904
0.30000	1.11600	1.11680	0.07168	1.24400	1.24720	0.25723
0.40000	1.11500	1.11300	0.17937	1.24200	1.23680	0.25765
0.50000	1.11000	1.10640	0.32432	1.23100	1.22410	0.56052
0.60000	1.10100	1.09520	0.52679	1.21100	1.19950	0.94963
0.70000	1.07400	1.07780	0.35382	1.15500	1.16170	0.58009
0.80000	1.04300	1.05110	0.77661	1.08900	1.10480	1.45087
0.90000	0.99000	1.00500	1.51515	0.98000	1.01000	3.06122
0.95000	0.95500	0.96034	0.55916	0.91200	0.92225	1.12390

TABLE 6. CALCULATED VELOCITY AND PRESSURE DISTRIBUTION FOR NACA 0018 AIRFOIL USING DIRECT METHOD

X/C	VEL (REF)	VEL (CAL)	% ERROR	PR (REF)	PR (CAL)	% ERROR
0.05000	1.22800	1.34040	9.15309	1.50700	1.79670	19.22362
0.07500	1.26400	1.31510	4.04272	1.59800	1.72960	8.23529
0.10000	1.27600	1.29940	1.83386	1.62800	1.68860	3.72236
0.15000	1.27800	1.27950	0.11737	1.63300	1.63710	0.25107
0.20000	1.27500	1.26480	0.80000	1.62500	1.59960	1.56308
0.25000	1.26200	1.25080	0.88748	1.59200	1.56460	1.72111
0.30000	1.24700	1.23610	0.87410	1.55600	1.52800	1.79949
0.40000	1.20500	1.20260	0.19917	1.45300	1.44620	0.46800
0.50000	1.15400	1.16430	0.89255	1.33100	1.35550	1.84072
0.60000	1.11600	1.12370	0.68996	1.24600	1.26260	1.33226
0.70000	1.07400	1.08320	0.85661	1.15300	1.17340	1.76930
0.80000	1.02500	1.04310	1.76585	1.05100	1.08800	3.52046
0.90000	0.96600	0.99223	2.71532	0.93300	0.98453	5.52304
0.95000	0.91400	0.94146	3.00438	0.83600	0.88635	6.02273

TABLE 7. CALCULATED SHAPE FOR NACA 0006 AIRFOIL USING INVERSE METHOD

X/C	Y/C (REF)	Y/C (CAL)	% ERROR
0.05000	0.01777	0.01775	0.09567
0.07500	0.02100	0.02086	0.67615
0.10000	0.02341	0.02320	0.88851
0.15000	0.02673	0.02649	0.89413
0.20000	0.02869	0.02853	0.56117
0.25000	0.02971	0.02966	0.17503
0.30000	0.03001	0.03006	0.17328
0.40000	0.02902	0.02914	0.41006
0.50000	0.02647	0.02643	0.15485
0.60000	0.02282	0.02243	1.71341
0.70000	0.01832	0.01755	4.18122
0.80000	0.01312	0.01213	7.53811
0.90000	0.00724	0.00634	12.37565
0.95000	0.00403	0.00329	18.28040

TABLE 8. CALCULATED SHAPE FOR NACA 0010-64 AIRFOIL USING INVERSE METHOD

X/C	Y/C (REF)	Y/C (CAL)	% ERROR
0.05000	0.02722	0.02535	6.85525
0.07500	0.03178	0.02992	5.85274
0.10000	0.03533	0.03353	5.10048
0.15000	0.04056	0.03907	3.68343
0.20000	0.04411	0.04313	2.22399
0.30000	0.04856	0.04814	0.87315
0.40000	0.05000	0.04969	0.61800
0.50000	0.04856	0.04809	0.95964
0.60000	0.04433	0.04351	1.86104
0.70000	0.03733	0.03610	3.30565
0.80000	0.02767	0.02611	5.63065
0.90000	0.01556	0.01390	10.64267
0.95000	0.00856	0.00712	16.81075

TABLE 9. CALCULATED SHAPE FOR NACA 0010-66 AIRFOIL USING INVERSE METHOD

X/C	Y/C (REF)	Y/C (CAL)	% ERROR
0.05000	0.02656	0.02599	2.14232
0.07500	0.03089	0.02941	4.78148
0.10000	0.03400	0.03200	5.87941
0.15000	0.03856	0.03602	6.59492
0.20000	0.04178	0.03927	5.99809
0.30000	0.04578	0.04459	2.61031
0.40000	0.04822	0.04845	0.47905
0.50000	0.04956	0.05046	1.81396
0.60000	0.05000	0.04997	0.06200
0.70000	0.04889	0.04619	5.52465
0.80000	0.04300	0.03808	11.43023
0.90000	0.02833	0.02405	15.11119
0.95000	0.01656	0.01386	16.31039

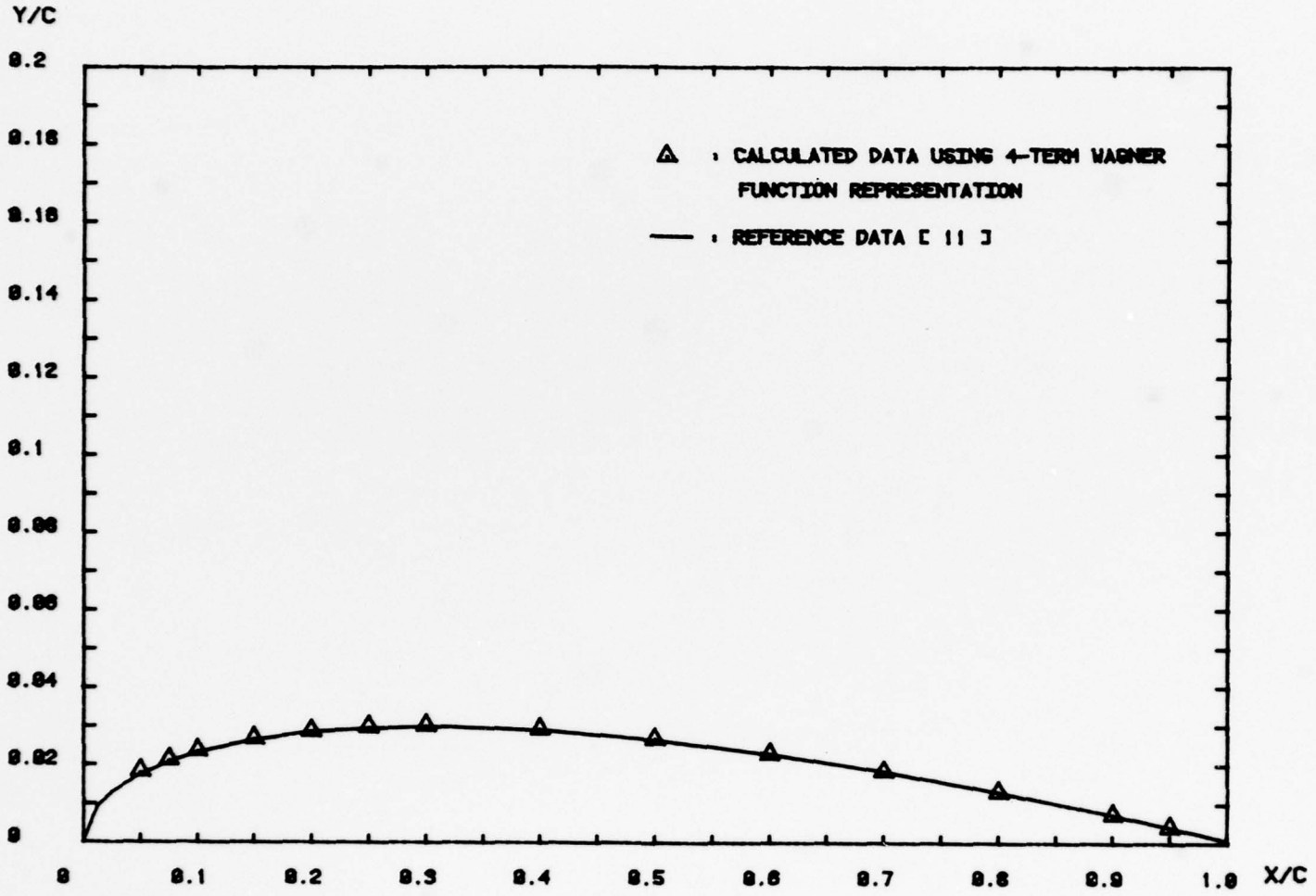

FIGURE 1. REPRESENTATION OF NACA 0006 AIRFOIL BY WAGNER FUNCTION SERIES

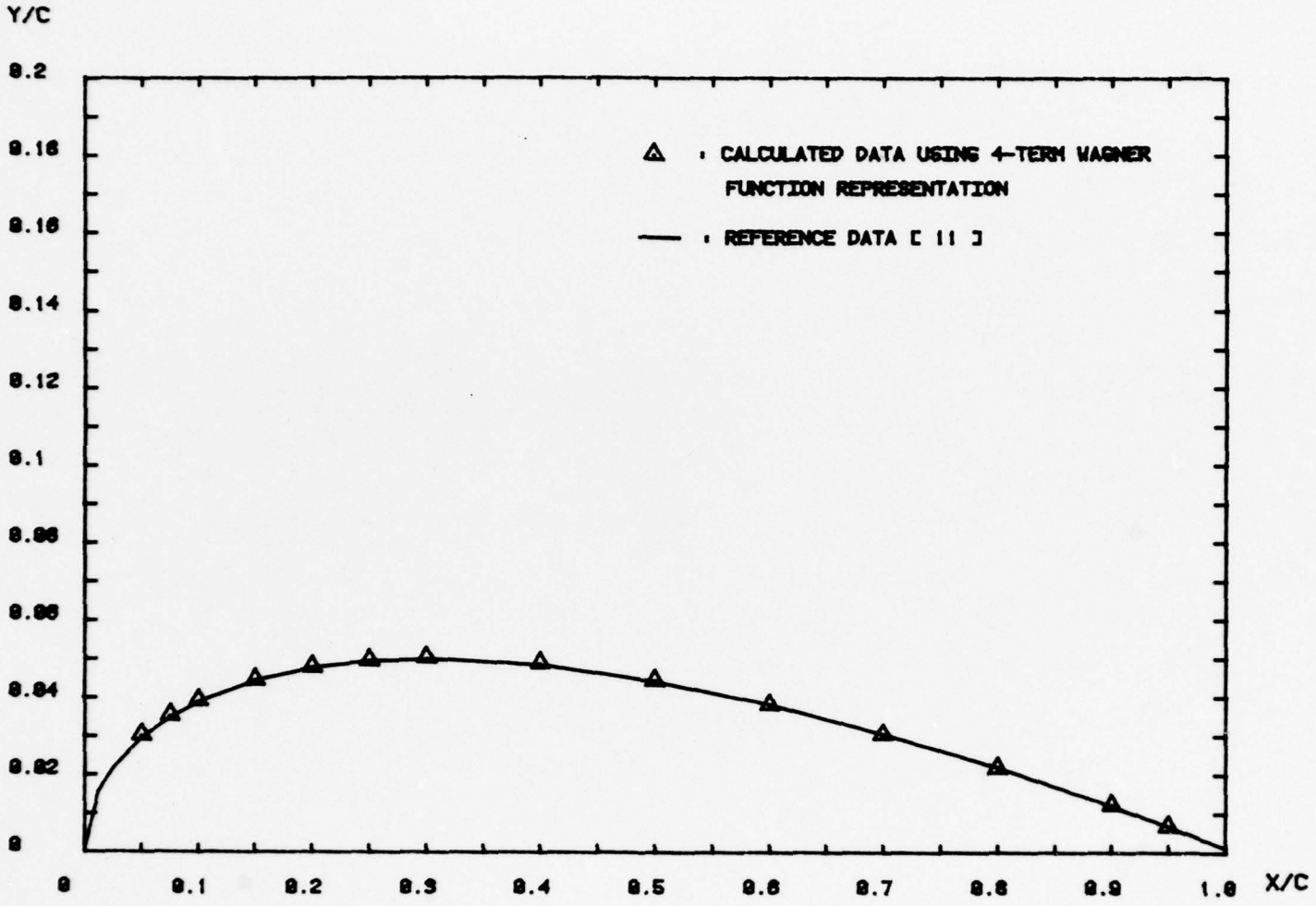

FIGURE 2. REPRESENTATION OF NACA 0010 AIRFOIL BY WAGNER FUNCTION SERIES

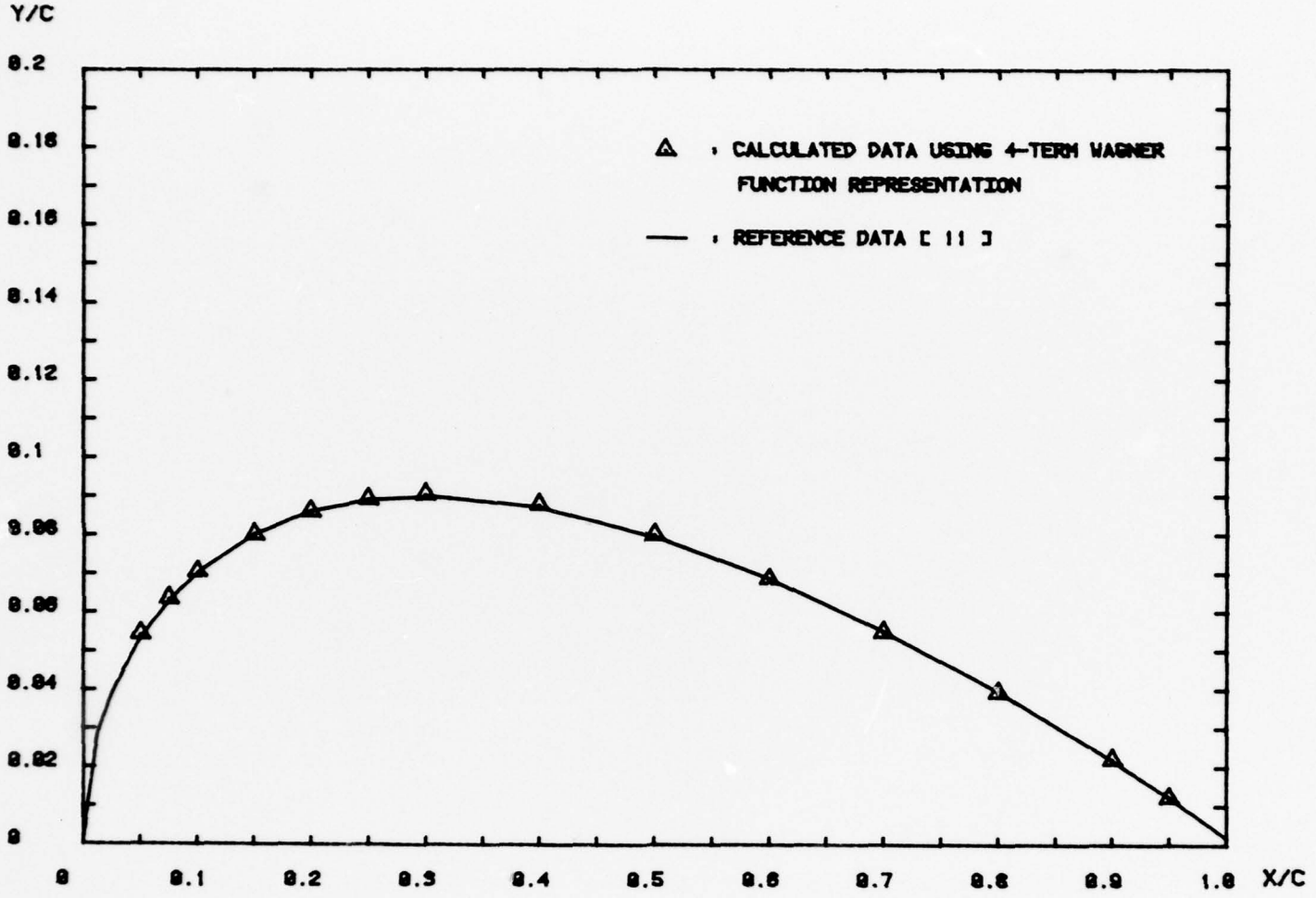

FIGURE 3. REPRESENTATION OF NACA 0016 AIRFOIL BY WAGNER FUNCTION SERIES

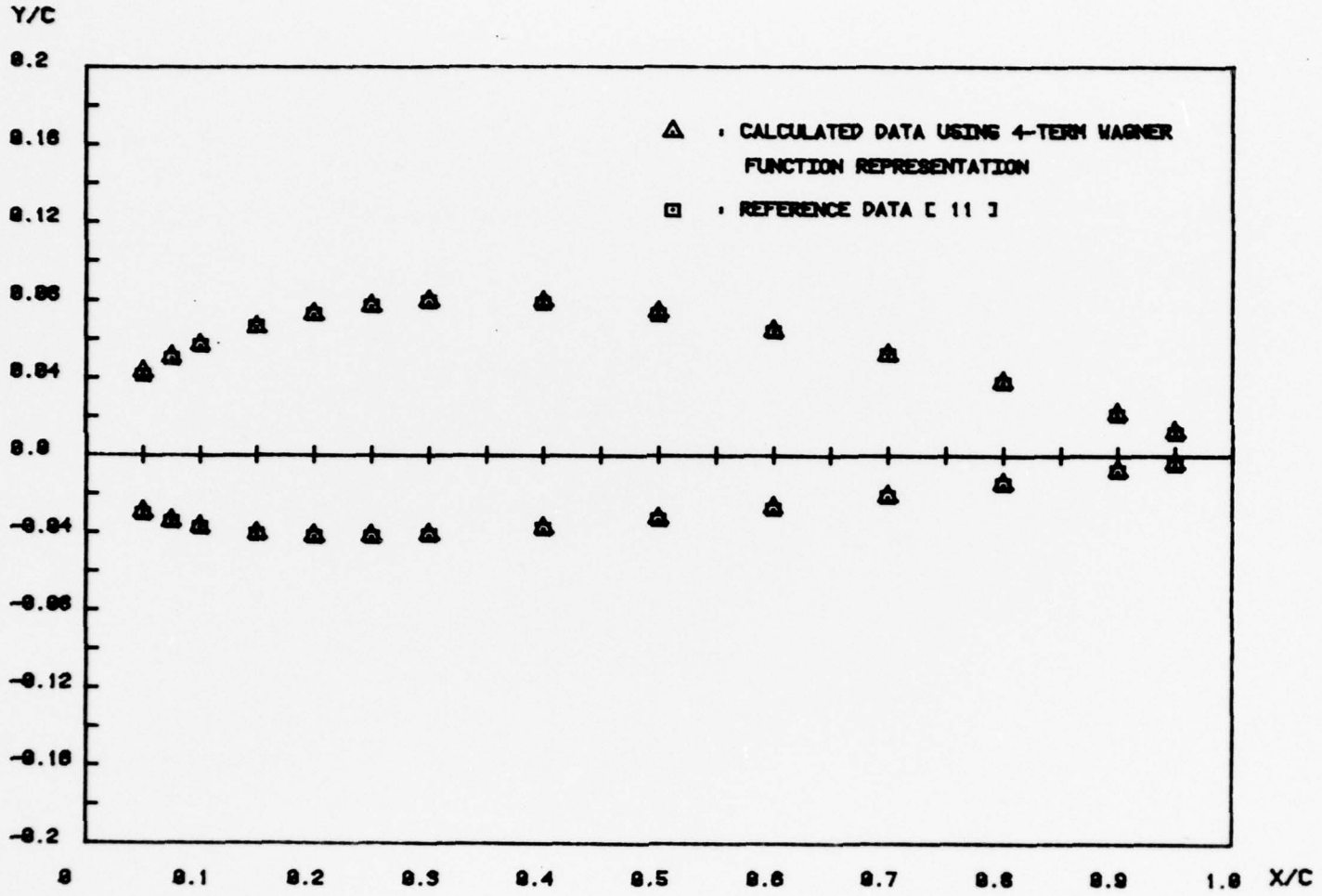

FIGURE 4. REPRESENTATION OF NACA 2412 AIRFOIL BY WAGNER FUNCTION SERIES

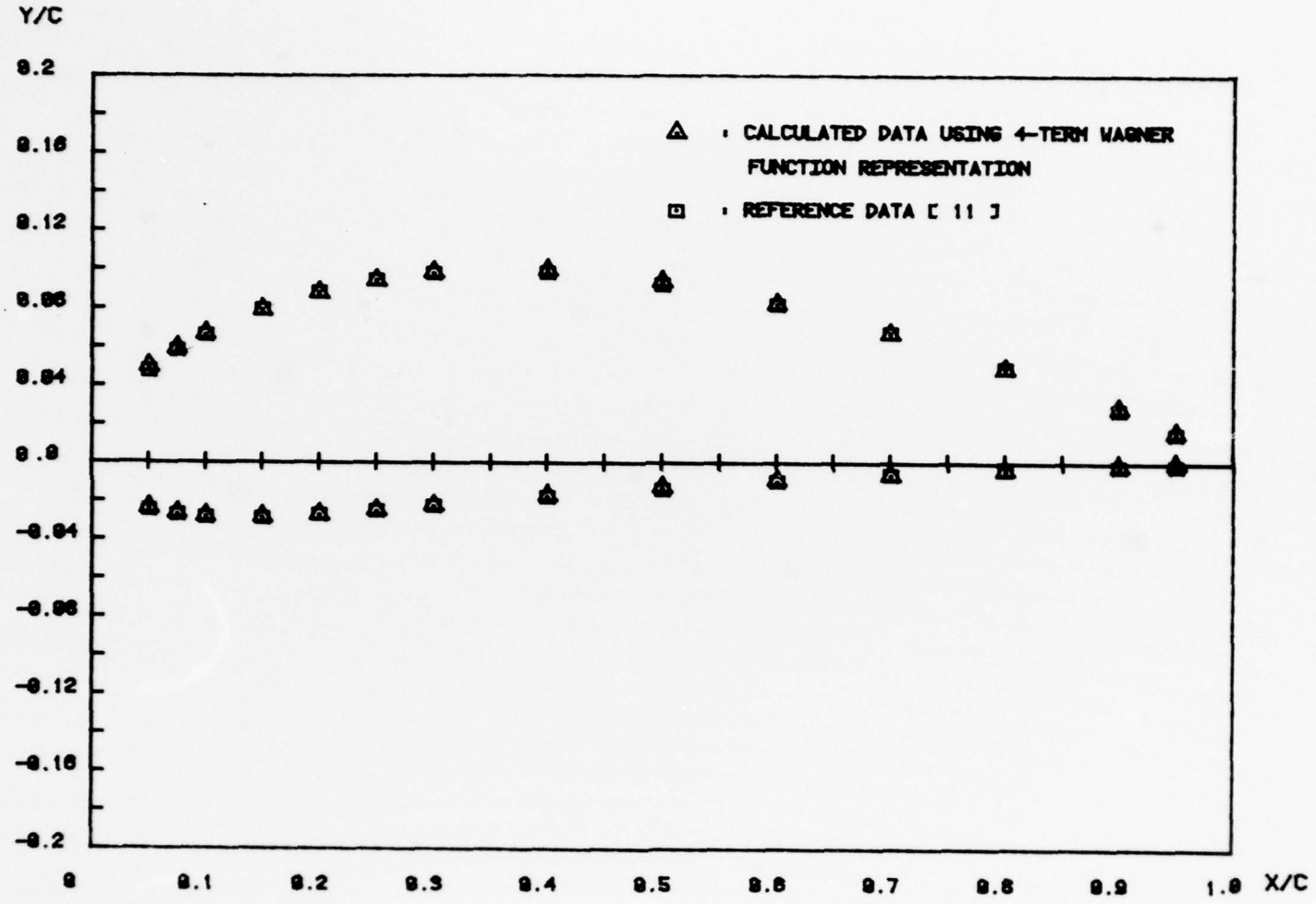

FIGURE 5. REPRESENTATION OF NACA 4412 AIRFOIL BY WAGNER FUNCTION SERIES

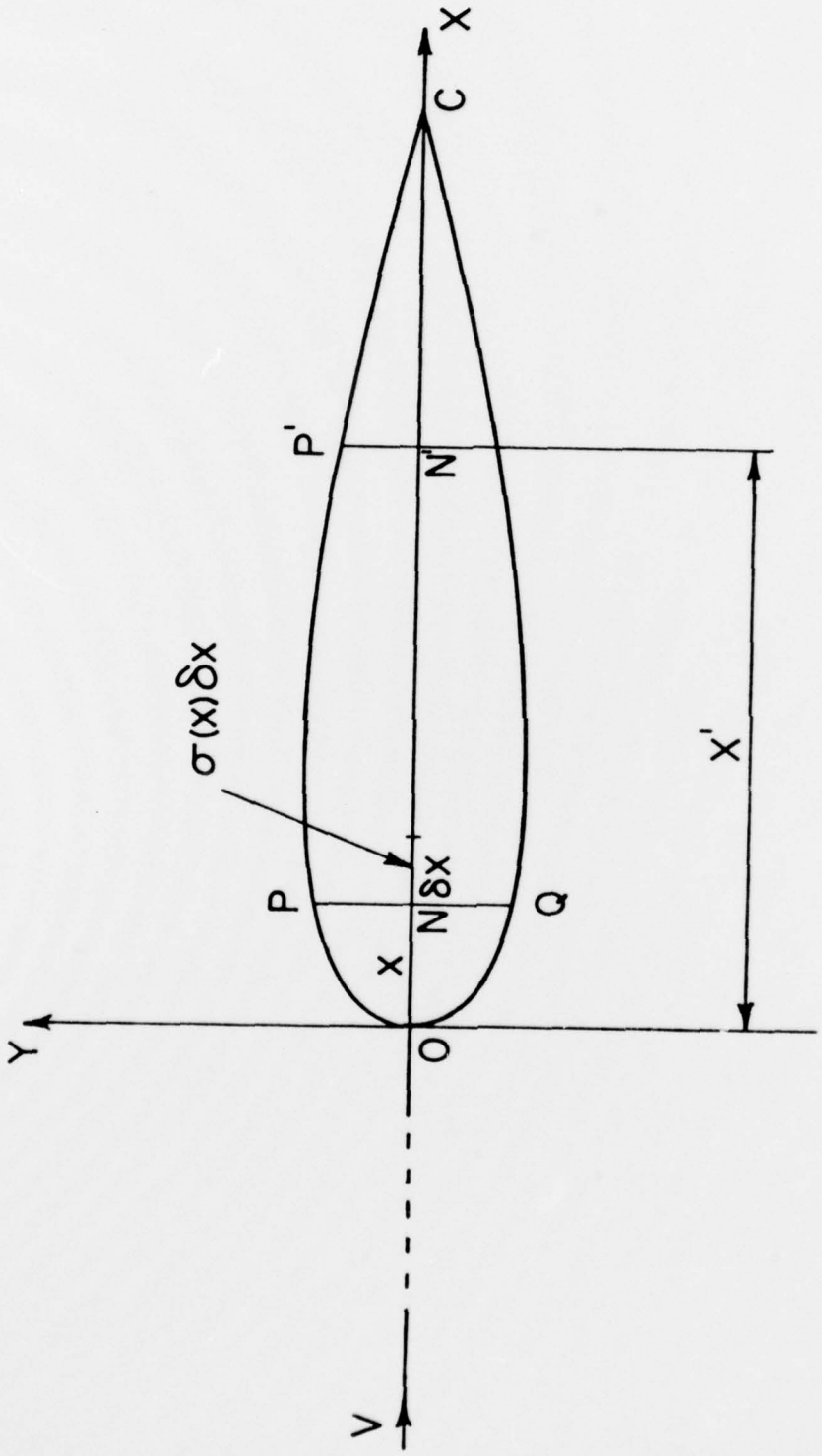

FIGURE 6. THIN SYMMETRICAL AIRFOIL AT ZERO INCIDENCE

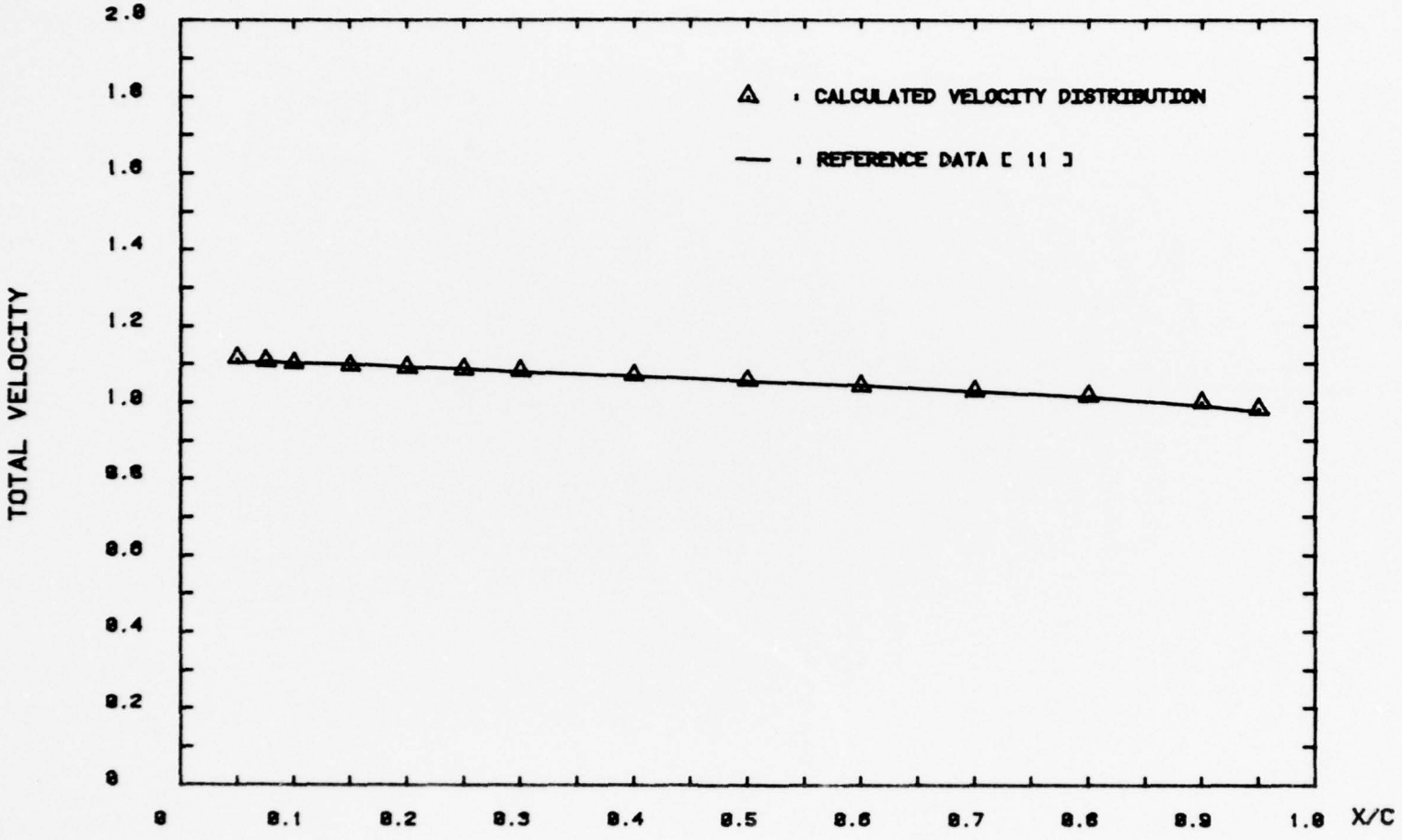

FIGURE 7. THE VELOCITY DISTRIBUTION FOR NACA 0006 AIRFOIL

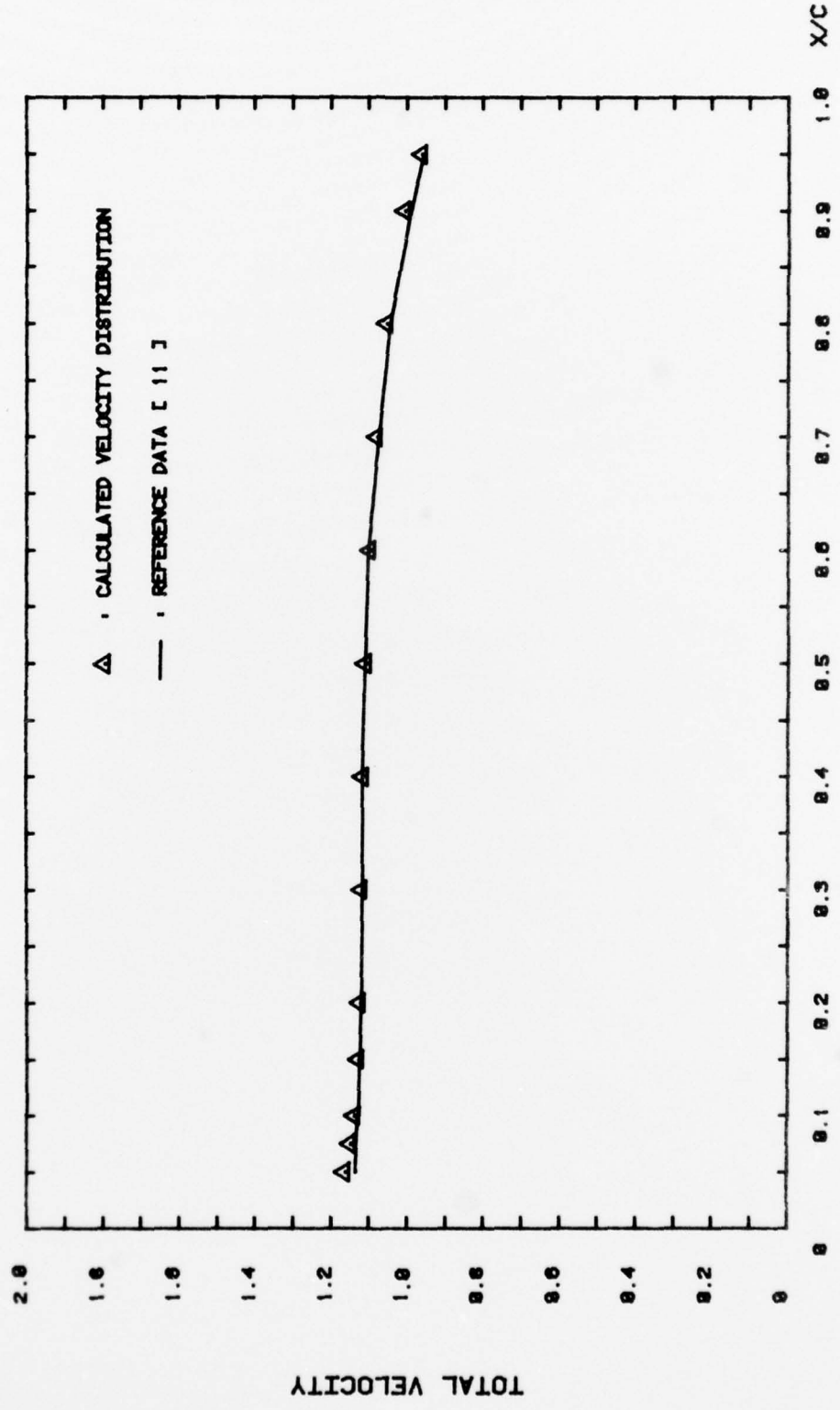

FIGURE 8. THE VELOCITY DISTRIBUTION FOR NACA 0010-64 AIRFOIL

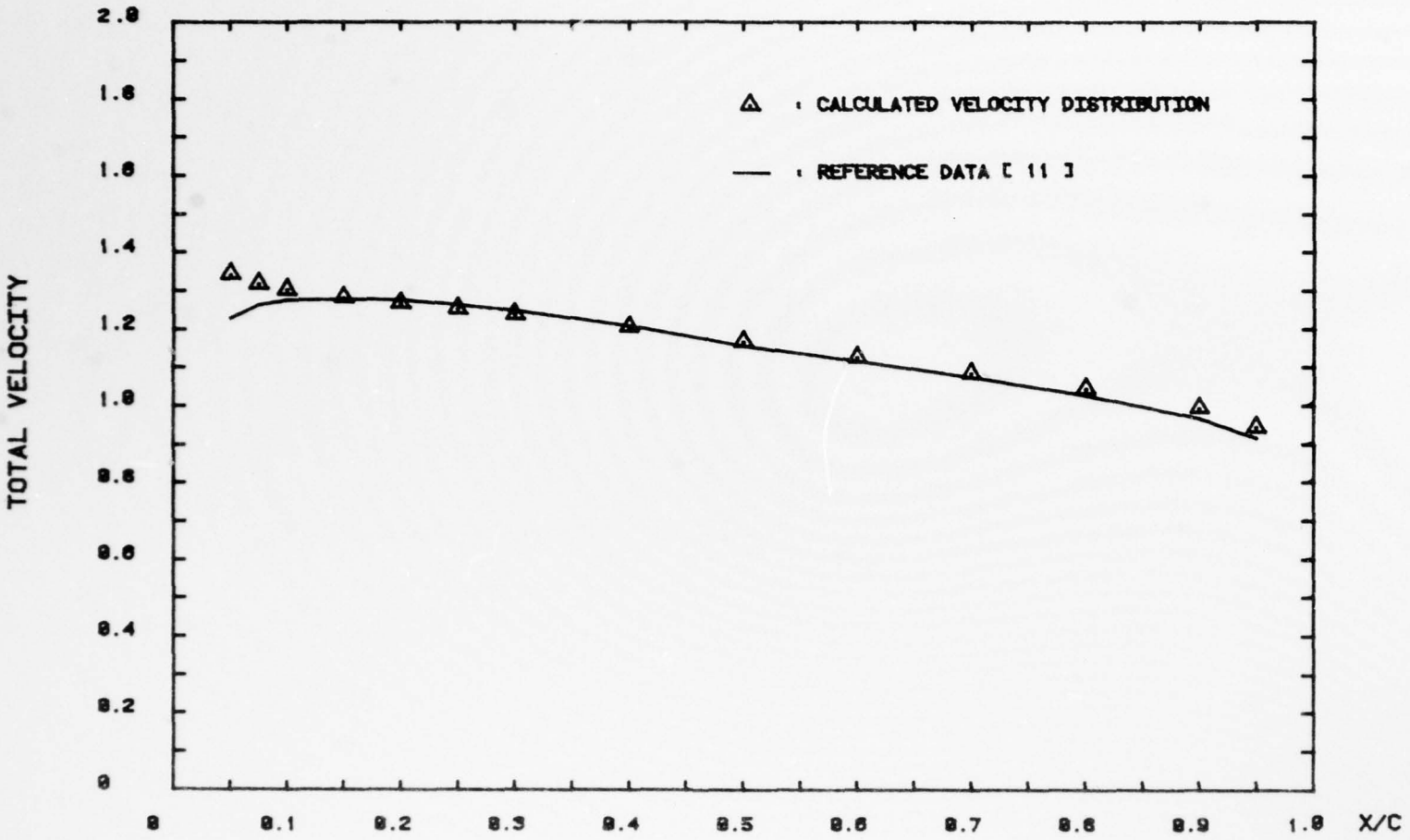

FIGURE 9. THE VELOCITY DISTRIBUTION FOR NACA 0018 AIRFOIL

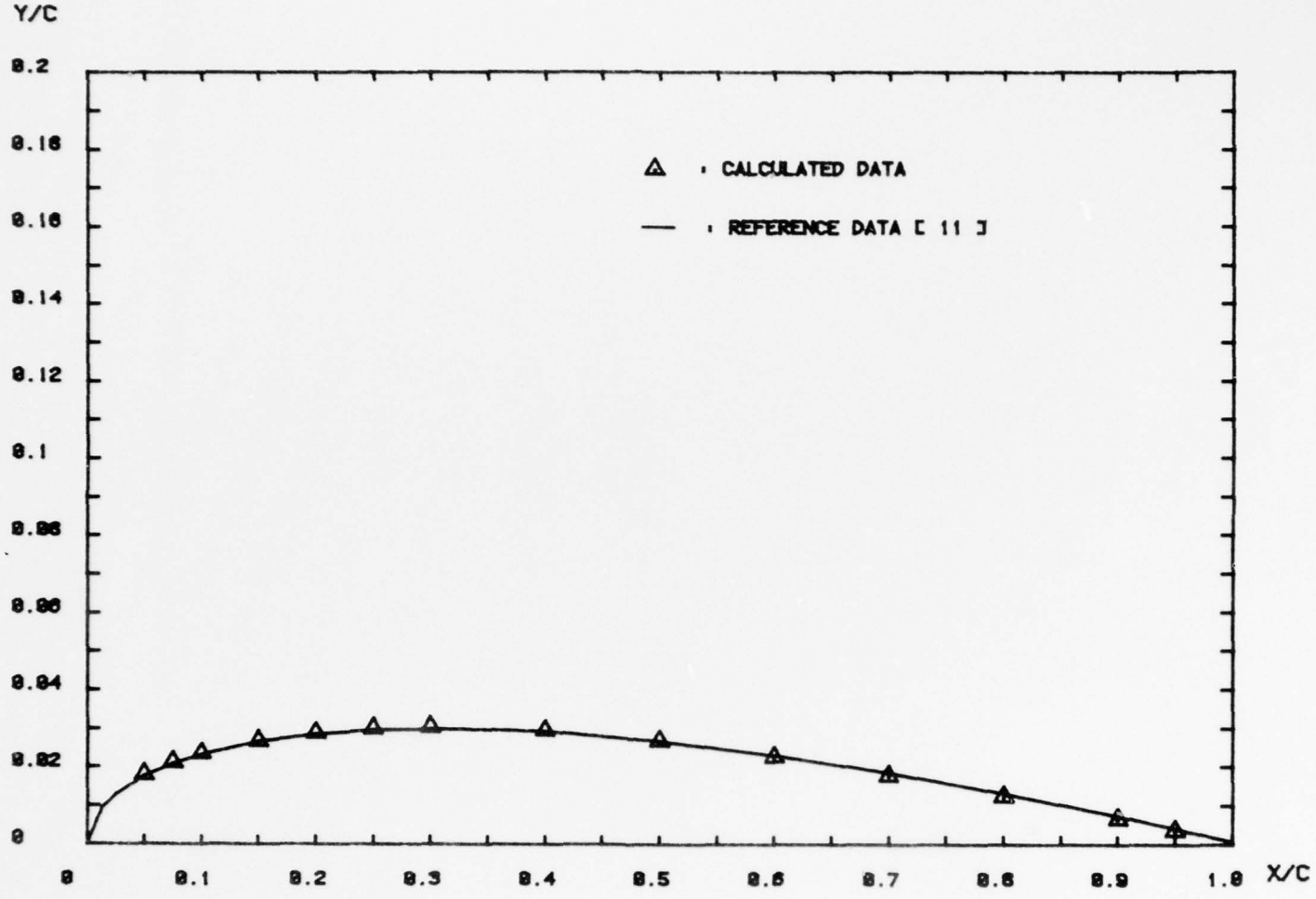

FIGURE 10. CALCULATED SHAPE FOR NACA 0006 AIRFOIL USING INVERSE METHOD

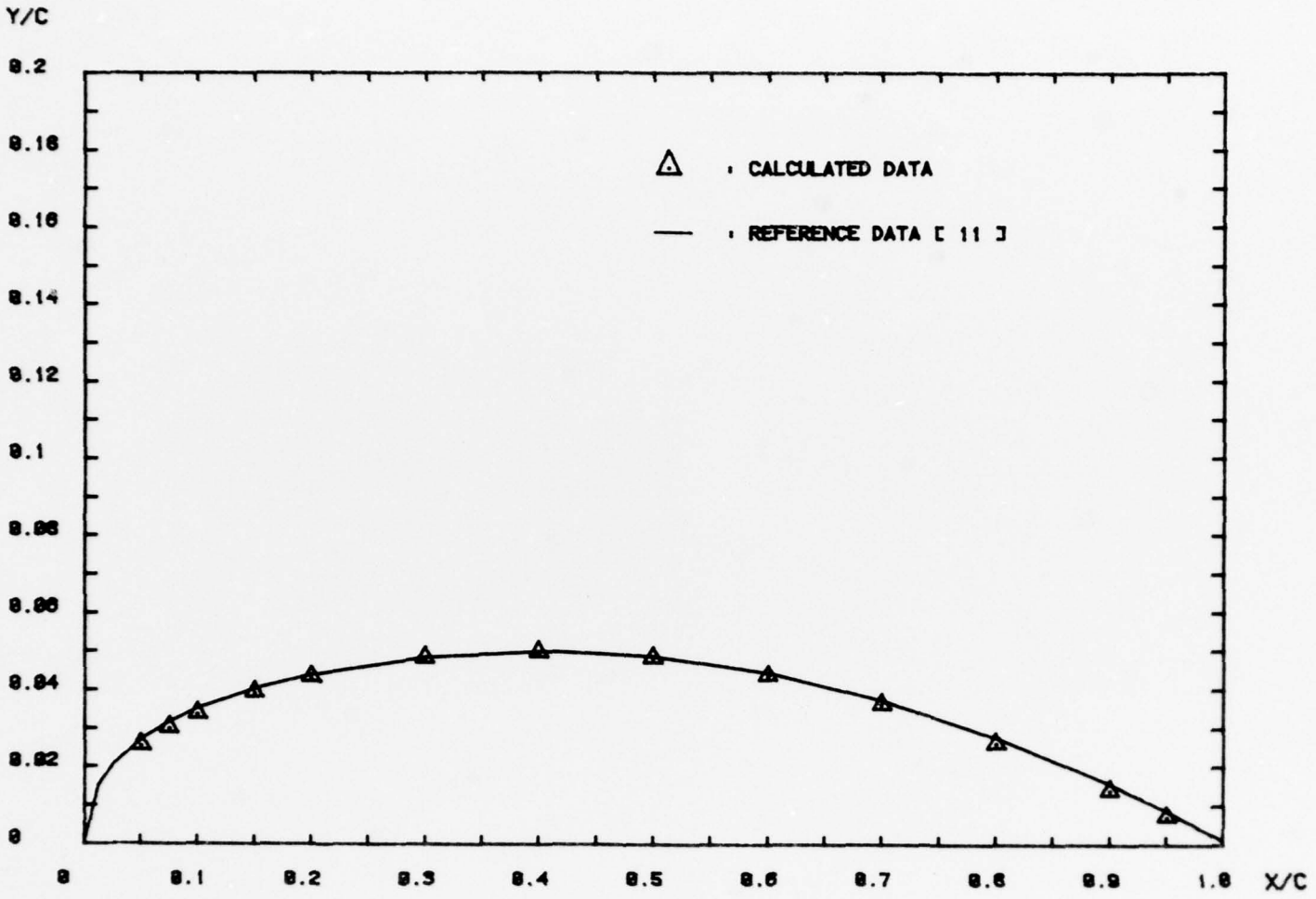

FIGURE 11. CALCULATED SHAPE FOR NACA 0010-64 AIRFOIL USING INVERSE METHOD

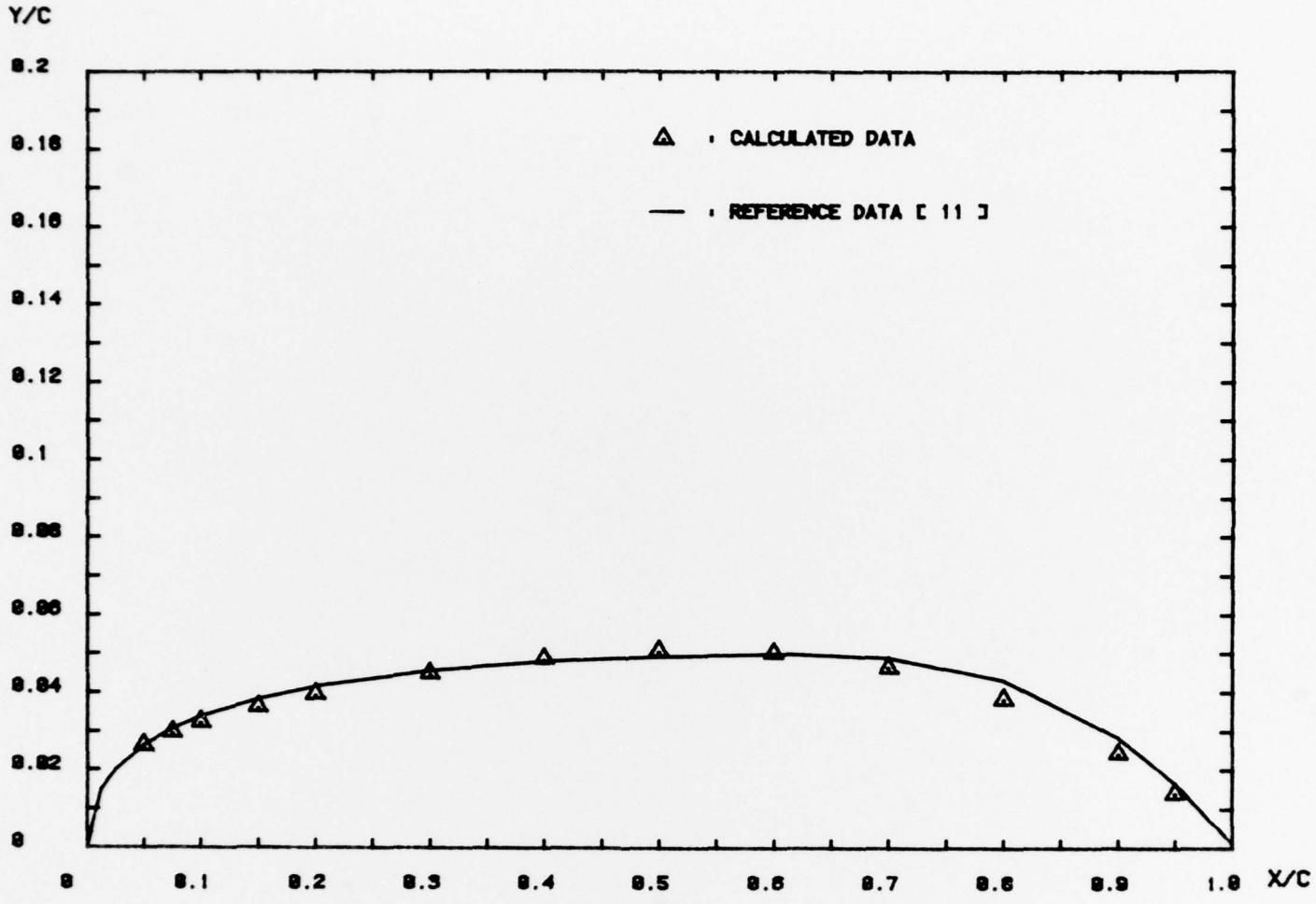

FIGURE 12. CALCULATED SHAPE FOR NACA 0010-66 AIRFOIL USING INVERSE METHOD